Review

Implementation of computer simulation to assess flow diversion treatment outcomes: systematic review and meta-analysis

Mingzi Zhang [ID],[1] Simon Tupin [ID],[1] Hitomi Anzai,[1] Yutaro Kohata [ID],[1] Masaaki Shojima [ID],[2] Kosuke Suzuki,[3] Yoshihiro Okamoto,[4] Katsuhiro Tanaka,[5] Takanobu Yagi,[6] Soichiro Fujimura,[7,8] Makoto Ohta [ID][1,9]

ABSTRACT

Introduction Despite a decade of research into virtual stent deployment and the post-stenting aneurysmal hemodynamics, the hemodynamic factors which correlate with successful treatment remain inconclusive. We aimed to examine the differences in various post-treatment hemodynamic parameters between successfully and unsuccessfully treated cases, and to quantify the additional flow diversion achievable through stent compaction or insertion of a second stent.

Methods A systematic review and meta-analysis were performed on eligible studies published from 2000 to 2019. We first classified cases according to treatment success (aneurysm occlusion) and then calculated the pooled standardized mean differences (SMD) of each available parameter to examine their association with clinical outcomes. Any additional flow diversion arising from the two common strategies for improving the stent wire density was quantified by pooling the results of such studies.

Results We found that differences in the aneurysmal inflow rate (SMD −6.05, 95% CI −10.87 to −1.23, p=0.01) and energy loss (SMD −5.28, 95% CI −7.09 to −3.46, p<0.001) between the successfully and unsuccessfully treated groups were indicative of statistical significance, in contrast to wall shear stress (p=0.37), intra-aneurysmal average velocity (p=0.09), vortex core-line length (p=0.46), and shear rate (p=0.09). Compacting a single stent could achieve additional flow diversion comparable to that by dual-stent implantation.

Conclusions Inflow rate and energy loss have shown promise as identifiers to discriminate between successful and unsuccessful treatment, pending future research into their diagnostic performance to establish optimal cut-off values.

INTRODUCTION

Computational fluid dynamics has been used for over a decade to assess the hemodynamics of intracranial aneurysms after flow diversion treatment.[1–6] This is because a favorable treatment outcome is largely associated with the efficacy of flow diversion produced by the implanted device; redirecting much of the aneurysmal inflow can 'weaken' the hemodynamic activity inside the sac, thereby promoting thrombosis and accelerating intracranial aneurysm occlusion.[7]

In view of this mechanism, a wide variety of hemodynamic parameters have been proposed to quantify the efficacy of flow-diverting (FD) stents: from those measuring reduction of the aneurysmal inflow strength (eg, aneurysmal inflow rate, intra-aneurysmal average velocity, mean aneurysm flow amplitude)[8–11] to those measuring weakening of the vascular pressure or stress (eg, wall shear stress, pressure drop),[2 12 13] and then to those characterizing changes in flow behavior within the aneurysm sac (eg, relative residence time, vortex core-line length).[8 14 15] Furthermore, many research groups have also attempted to establish hemodynamic identifiers of a successful treatment,[4 9 12 13 16–19] although no consensus has yet been reached.

Owing to the development of virtual stenting techniques,[6 20 21] computational fluid dynamics has also been adopted to investigate the changes in aneurysm hemodynamics following various strategies or maneuvers exercised intra-operatively to enhance the flow diversion, in particular stent compaction and multiple stent deployment. Despite a number of simulation studies having confirmed the effectiveness of these approaches in enhancing the flow diversion,[3 18 19 22] it remains inconclusive as to how much further an additional stent or a stent compaction technique can decrease the aneurysmal inflow.

In the present work we performed a pooled analysis of eligible studies on the aneurysmal hemodynamics after virtual stent treatment, seeking to (1) identify hemodynamic parameters that may be most suggestive of a favorable treatment outcome and (2) quantify the likely additional flow diversion achievable through a stent compaction technique or insertion of an additional stent.

METHODS
Study selection

We conducted the systematic review and meta-analysis in accordance with the PRISMA guidelines. A search for the keyword terms "computational fluid dynamics", "haemodynamics" or "hemodynamics", in combination with "aneurysm(s)", "flow-diverter(s)" or "flow-diverting stent(s)" was performed using PubMed, Medline, and Scopus
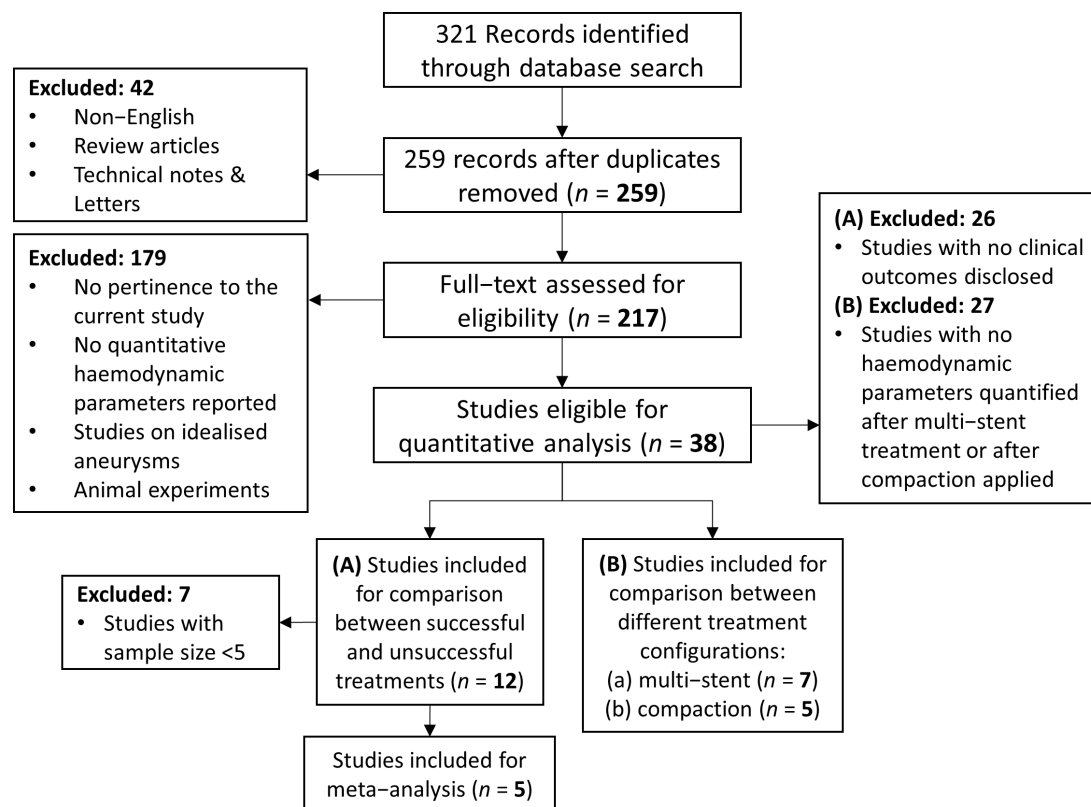
Figure 1 Strategy used for literature search and the number of studies included in each analysis.

for articles published in the period from 1 January 2000 to 31 December 2019. From the identified studies, review articles, articles that were written in languages other than English, technical notes, and letters were immediately excluded.

For the remaining articles, three authors (MZ, ST, and MO) independently examined the full text before reaching an agreement on their eligibility to be included in our quantitative analysis according to the following criteria: (1) human aneurysm subjects were included; (2) paired pre- and post-stenting hemodynamic parameters were quantified; and (3) clinical outcomes following a treatment were disclosed (if it was to be analysed for the correlation between hemodynamic changes and clinical outcomes). When serial studies existed describing the results of an overlapping set of subjects, only the most recent one was retained (see figure 1 for the literature search strategy used to screen papers for our quantitative analyses).

Data extraction and normalization
For quantitative analysis we extracted data including (1) name of the first author, (2) year of publication, (3) aim and design of the study, (4) number, type, size, and location of the aneurysms, (5) type of the stents and strategy used for virtual deployments, and (6) all available pre- and post-treatment hemodynamic parameters. These parameters included the aneurysmal inflow rate (IR), intra-aneurysmal average velocity (AAV) and maximal velocity (MAV), average shear strain rate (SR) of blood flow within the aneurysms, energy loss (EL), pressure drop (PD), aneurysmal wall shear stress (WSS) and vortex core-line length (VCL), the relative residence time (RRT) and turnover time (TUT), and transition time (TRT). Two authors (HA and YK) independently performed data extraction, the results of which were consistent.

As the extracted data were reported in various units and formats across different studies, a data normalization procedure

was carried out to ensure validity of between-study comparisons of the hemodynamic outcomes of the treatments. Paired hemodynamic parameters in physical units before (P_{pre}) and after (P_{post}) treatment respectively in the forms of

$$P_{pre} = m_{pre} \pm SD_{pre} \text{ and } P_{post} = m_{post} \pm SD_{post} \quad (1)$$

were converted into a normalized reduction $R\,(\%)$ in relation to the untreated condition:

$$R\,(\%) = m_r \pm SD_r \quad (2)$$

where m_r and SD_r denote the mean and SD of the normalized reduction, which were respectively calculated as[23]

$$m_r = \frac{m_{post}}{m_{pre}} \times 100\% , \quad (3)$$

and

$$SD_r = \frac{\sqrt{m_{pre}^2 \cdot SD_{post}^2 + m_{post}^2 \cdot SD_{pre}^2}}{m_{post}^2} \times 100\% . \quad (4)$$

Statistical analysis
Statistical analyses were performed using MedCalc version 19.1 (Ostend, Belgium), with GNU Octave 4.4.1 (John W Eaton *et al*, USA) being a supplementary tool. For systematic comparisons between the successfully and unsuccessfully treated groups, we first performed a Shapiro–Wilk test to check for normality of the continuous data, and then an independent Student t-test for normally distributed data or a Mann–Whitney U test for non-normally distributed data. For comparison of hemodynamic changes between various treatment configurations (ie, treatments with single or with dual FD stents, and treatments with or without a stent compaction technique applied), a paired-sample two-sided t-test was used. Throughout the comparisons p<0.05 was considered suggestive of statistical significance, while p<0.005 was deemed to confirm statistical significance.

A meta-analysis was performed to explore the standardized mean difference (SMD) of six hemodynamic parameters (IR, AAV, EL, VCL, WSS, and SR) between the successfully and unsuccessfully treated groups. Both fixed-effects and random-effects models were used in each analysis, with a Cochran Q test employed to examine the between-study heterogeneity. If a test had suggested significant heterogeneity between studies, results corresponding to a random-effects model were adopted, otherwise results corresponding to a fixed-effects model were adopted. We used funnel plots and Egger's test to examine the publication bias, with p<0.05 being an indication of statistical significance.

RESULTS

Our database search yielded 259 studies after duplicates were removed, of which 38 were deemed eligible for further quantitative analysis.

For systematic analysis of the correlation between hemodynamic and clinical outcomes, 12 studies (involving a total of 153 aneurysms) with clinical outcomes disclosed were included. Of the 12 studies, five with aneurysm sample size greater than five were later included in the meta-analysis (see table 1 for a summary of the studies). We observed no substantial asymmetry in the funnel plots of studies that reported IR or AAV, and Egger's tests did not suggest the existence of publication bias (p=0.78 and p=0.89 for IR and AAV, respectively).

Of the 38 studies, 11 met the inclusion criteria for quantifying the improvements of flow diversion achieved by two respective wire density enhancement techniques—stent compaction (7/11) and dual-stent implantation (5/11) (see online supplemental material 1 for a list of those studies, online supplemental table 1 for a summary, and online supplemental table 2 for details of the normalized hemodynamic parameters extracted from those studies).

Hemodynamic differences between successfully and unsuccessfully treated cases

Quantitative comparison

Our quantitative analyses of 12 studies suggest that the differences in IR (p=0.0063) and EL (p=0.0237) between the successfully and unsuccessfully treated aneurysms were suggestive of statistical significance. However, no statistically significant differences were found for AAV (p=0.2881) or WSS (p=0.8280) (see online supplemental figure 1 for the detailed quantifications and online supplemental material 2 for an additional logistic regression analysis).

Meta-analysis

Consistent with the findings of the quantitative comparison, our meta-analysis of five studies (including a total of 138 aneurysms) shows the differences in normalized IR (SMD −6.05, 95% CI −10.865 to −1.225, p=0.01) and EL (SMD −5.28, 95% CI −7.092 to −3.459, p<0.001) are indicative of statistical significance, in contrast to AAV (SMD −3.22 95% CI −6.985 to 0.537, p=0.09) and WSS (SMD 0.34, 95% CI −0.411 to 1.083, p=0.37) (figure 2 and table 1).

Improvement of flow diversion obtained by increased stent wire density

Table 2 summarizes the improvements in intra-aneurysmal flow reduction obtained by enhancement of the stent wire density across the aneurysm orifice. Our systematic review suggests that overlapping two stents and compacting a single stent can each

markedly improve the flow diversion efficacy, further reducing the IR by 14.4±5.6% (95% CI 9.3% to 19.6%, p=0.0005) and 16.0±11.3% (95% CI 6.7% to 25.4%, p=0.0051), respectively, and the AAV by 16.8±8.7% (95% CI 10.1% to 23.5%, p=0.0004) and 23.3±14.4% (95% CI 8.3% to 38.4%, p=0.0105) compared with the standard deployment of a single stent. However, the increase of normalized TUT induced by stent compaction was not suggestive of statistical significance (p=0.0791), in contrast to that induced by overlapping stents (p=0.0247) (see online supplemental figures 2 and 3 for statistics on the hemodynamic changes attributable to increasing the stent wire density across the aneurysm orifice).

DISCUSSION

IR and EL reduction might be suggestive of a successful treatment

Our quantitative comparison suggests that only differences in the normalized IR and EL reductions between the successfully and unsuccessfully treated groups were suggestive of statistical significance, and this finding agrees with our meta-analysis.

IR is a so-called 'bulk' hemodynamic parameter measuring the entire quantity of blood flow entering the aneurysm. Strength and angle of the aneurysm inflow have direct impact on the complexity and stability of flow within the aneurysm sac, which are believed to be closely associated with aneurysm occlusion or rupture.[7 13] As a parameter originally proposed to quantify the hemodynamic effects of different anastomosis modes in cardiovascular surgery, EL measures differences in the dynamic pressure and kinetic energy between the aneurysmal inflow and outflow. Being able to immediately quantify the weakening of intra-aneurysmal flow activity, IR and EL have both been proposed as identifiers of a fast aneurysm occlusion; however, differing conclusions were previously reported regarding their association with clinical outcomes.

Paliwal et al[16] reported that, superior to bulk hemodynamic parameters (ie, IR (p=0.10) and AAV (p=0.34)), localised parameters (ie, EL and VCL (both p<0.00)) were more sensitive in capturing the complex intra-aneurysmal flow behaviors, which are likely to manifest greater disruption in successfully treated intracranial aneurysms (table 1). Interestingly, in another study[8] that involved more aneurysm samples (n=84), reductions of the IR, AAV, and SR were all found to be statistically different (all p<0.00), in contrast to TUT (p=0.47), a parameter measuring the average period of time during which fluid particles remain within the aneurysm sac. Chong et al[9] and Mut et al[13] also reported the difference in IR to be statistically significant (both p<0.00), although the former found that the difference in EL between the successful and unsuccessful cases was about three times that of IR.

Animal experiments showed a similar tendency when hemodynamic parameters were used to predict complete aneurysm occlusion. A study of 36 elastase-induced aneurysms in rabbits reported statistically significant differences in IR (p<0.03) and kinetic energy (p<0.05) between fast and slow aneurysm occlusion, in contrast to that of AAV (p=0.06), regardless of aneurysm size.[14] Moreover, their follow-up research into the intra-aneurysmal hemodynamics showed that AAV and SR in the patent regions were about 2.8 times larger than those in the occluded regions (p<0.00),[7] suggesting the usefulness of AAV and SR in predicting localized thrombosis formation.

In accordance with our review of studies on human subjects, together with the findings from animal experiments, IR and EL have shown promise as discriminators between favorable and unfavorable clinical outcomes prior to a real flow diversion

Table 1 Study information and normalized reductions relative to the untreated condition of hemodynamic parameters summarized from studies included in the meta-analysis and systematic review for differences between successfully and unsuccessfully treated cases

Author, year	No. of IAs	No. of Succ.	IA type	IA location	AR (SD)	Criterion	FD stent model	Virtual stenting technique	IR reduction (SD) S	U	P value	AAV reduction (SD) S	U	P value
Paliwal et al,[8] 2018	84	63	SW	ICA	0.98 (0.17)	CO @6mo	PED	Paliwal et al[33],	0.39 (0.01)	0.59 (0.03)	<0.00*	0.29 (0.01)	0.48 (0.04)	<0.00*
Paliwal et al,[16] 2017	15	10	SW	—	—	CO @12mo	PED	Paliwal et al[33]	0.60 (0.03)	0.66 (0.10)	0.1	0.48 (0.03)	0.51 (0.09)	0.34
Mut et al,[13] 2014	23	15	SW	1 ACOM, 7 ICA (OPH), 10 ICA (CAV), 4 PCOM, ICA (SUP),	10.02 (4.74)	CO @3mo	PED	Mut et al,[34]	0.32 (0.02)	0.72 (0.25)	<0.00*	0.14 (0.02)	0.30 (0.08)	<0.00*
Chong et al,[9] 2014	8	4	SW	5 ICA (SUP); 2 ICA (CAV), 1 Base of skull;	2.39 (0.83)	CO @6mo	Silk	Porous Medium[35]	0.09 (0.02)	0.50 (0.05)	<0.00*	—	—	—
Kulcsár et al,[12] 2012	8	6	SW	ICA	2.08 (1.21)	CO @12mo	Silk	Rhinoceros[12]	—	—	—	0.56 (0.26)	0.60 (0.20)	0.84
Total†	149	99			3.37 (4.96)				0.27 (0.13)	0.35 (0.20)	0.01‡	0.51 (0.15)	0.41 (0.27)	0.29

Author, year	WSS reduction (SD) S	U	P value	SR reduction (SD) S	U	P value	VCL reduction (SD) S	U	P value	TRT increase (SD) S	U	P value	EL Reduction (SD) S	U	P value	TUT increase (SD) S	U	P value
Paliwal et al,[8] 2018	—	—	—	0.29 (0.02)	0.50 (0.04)	<0.00*	—	—	—	—	—	—	—	—	—	2.55 (0.07)	2.56 (0.02)	0.47
Paliwal et al,[16] 2017	—	—	—	—	—	—	0.62 (0.03)	0.90 (0.10)	<0.00*	—	—	—	0.57 (0.03)	0.89 (0.10)	<0.00*	—	—	—
Mut et al,[13] 2014	0.27 (0.33)	0.17 (0.02)	0.38	0.17 (0.06)	0.27 (0.02)	<0.00*	11.29 (10.14)	6.46 (1.21)	0.2	6.00 (1.49)	3.93 (0.93)	0.00*	—	—	—	—	—	—
Chong et al,[9] 2014	—	—	—	—	—	—	—	—	—	—	—	—	0.02 (0.01)	0.43 (0.11)	<0.00*	—	—	—
Kulcsár et al,[12] 2012	0.42 (0.15)	0.36 (0.04)	0.6	—	—	—	—	—	—	—	—	—	—	—	—	—	—	—
Total†	0.38 (0.20)	0.41 (0.15)	0.83										0.42 (0.27)	0.15 (0.19)	0.02‡			

*Statistical significance confirmed (p<0.005).

†The total counts for number of aneurysms and number of successful cases have included seven additional studies that were not included in the final meta-analysis due to their limited sample size, and the corresponding hemodynamic parameters are averages of those from studies (n=12) included in the systematic review.

‡Suggestive of statistical significance (p<0.05).

AAV, intra-aneurysmal average velocity; ACOM, anterior communicating artery; AR, aspect ratio; CAV, cavernous; CO, complete occlusion; EL, energy loss; IA, intracranial aneurysm; ICA, internal carotid artery; IR, inflow rate; OPH, ophthalmic; PCOM, posterior communicating artery; S, successful; SR, shear rate; Succ, successful cases; SUP, supraclinoid; SW, side-wall; TRT, transition time; TUT, turnover time; U, unsuccessful; VCL, vortex coreline length; WSS, wall shear stress.
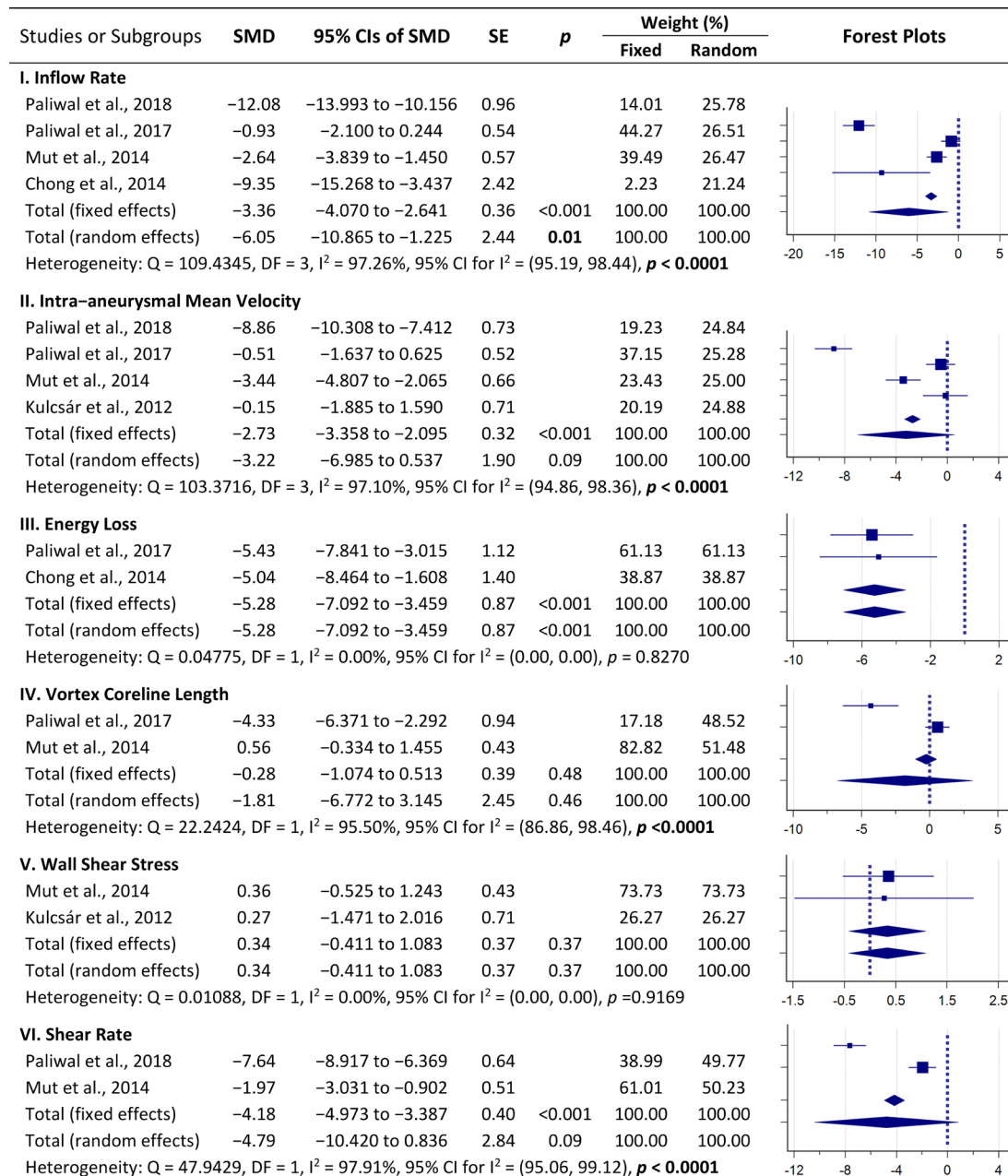
Studies or Subgroups	SMD	95% CIs of SMD	SE	p	Weight (%) Fixed	Weight (%) Random	Forest Plots
I. Inflow Rate							
Paliwal et al., 2018	−12.08	−13.993 to −10.156	0.96		14.01	25.78	
Paliwal et al., 2017	−0.93	−2.100 to 0.244	0.54		44.27	26.51	
Mut et al., 2014	−2.64	−3.839 to −1.450	0.57		39.49	26.47	
Chong et al., 2014	−9.35	−15.268 to −3.437	2.42		2.23	21.24	
Total (fixed effects)	−3.36	−4.070 to −2.641	0.36	<0.001	100.00	100.00	
Total (random effects)	−6.05	−10.865 to −1.225	2.44	**0.01**	100.00	100.00	
Heterogeneity: Q = 109.4345, DF = 3, I² = 97.26%, 95% CI for I² = (95.19, 98.44), *p* < 0.0001							
II. Intra–aneurysmal Mean Velocity							
Paliwal et al., 2018	−8.86	−10.308 to −7.412	0.73		19.23	24.84	
Paliwal et al., 2017	−0.51	−1.637 to 0.625	0.52		37.15	25.28	
Mut et al., 2014	−3.44	−4.807 to −2.065	0.66		23.43	25.00	
Kulcsár et al., 2012	−0.15	−1.885 to 1.590	0.71		20.19	24.88	
Total (fixed effects)	−2.73	−3.358 to −2.095	0.32	<0.001	100.00	100.00	
Total (random effects)	−3.22	−6.985 to 0.537	1.90	0.09	100.00	100.00	
Heterogeneity: Q = 103.3716, DF = 3, I² = 97.10%, 95% CI for I² = (94.86, 98.36), *p* < 0.0001							
III. Energy Loss							
Paliwal et al., 2017	−5.43	−7.841 to −3.015	1.12		61.13	61.13	
Chong et al., 2014	−5.04	−8.464 to −1.608	1.40		38.87	38.87	
Total (fixed effects)	−5.28	−7.092 to −3.459	0.87	<0.001	100.00	100.00	
Total (random effects)	−5.28	−7.092 to −3.459	0.87	<0.001	100.00	100.00	
Heterogeneity: Q = 0.04775, DF = 1, I² = 0.00%, 95% CI for I² = (0.00, 0.00), p = 0.8270							
IV. Vortex Coreline Length							
Paliwal et al., 2017	−4.33	−6.371 to −2.292	0.94		17.18	48.52	
Mut et al., 2014	0.56	−0.334 to 1.455	0.43		82.82	51.48	
Total (fixed effects)	−0.28	−1.074 to 0.513	0.39	0.48	100.00	100.00	
Total (random effects)	−1.81	−6.772 to 3.145	2.45	0.46	100.00	100.00	
Heterogeneity: Q = 22.2424, DF = 1, I² = 95.50%, 95% CI for I² = (86.86, 98.46), *p* <0.0001							
V. Wall Shear Stress							
Mut et al., 2014	0.36	−0.525 to 1.243	0.43		73.73	73.73	
Kulcsár et al., 2012	0.27	−1.471 to 2.016	0.71		26.27	26.27	
Total (fixed effects)	0.34	−0.411 to 1.083	0.37	0.37	100.00	100.00	
Total (random effects)	0.34	−0.411 to 1.083	0.37	0.37	100.00	100.00	
Heterogeneity: Q = 0.01088, DF = 1, I² = 0.00%, 95% CI for I² = (0.00, 0.00), p =0.9169							
VI. Shear Rate							
Paliwal et al., 2018	−7.64	−8.917 to −6.369	0.64		38.99	49.77	
Mut et al., 2014	−1.97	−3.031 to −0.902	0.51		61.01	50.23	
Total (fixed effects)	−4.18	−4.973 to −3.387	0.40	<0.001	100.00	100.00	
Total (random effects)	−4.79	−10.420 to 0.836	2.84	0.09	100.00	100.00	
Heterogeneity: Q = 47.9429, DF = 1, I² = 97.91%, 95% CI for I² = (95.06, 99.12), *p* < 0.0001							

Figure 2 Meta-analysis of standardized mean differences (SMD) of six different hemodynamic parameters (I–VI) and clinical treatment outcomes using both the fixed-effects and the random-effects models. The forest plots show SMDs of each of these parameters obtained from both the fixed-effects (upper rhombus) and the random-effects (lower rhombus) models.

treatment, pending further investigation into their diagnostic performance to identify the optimal cut-off thresholds.

Additional flow diversion achievable through enhancement of stent wire density

In addition to deployment of an additional stent, a 'push-and-pull' technique to be used during the stent-releasing process has been promoted to enhance the local wire density. Shapiro et al[24] first demonstrated in benchtop experiments that increased wire density can be attained through longitudinal compaction of a single stent. Damiano et al[22] later reported in a hemodynamic study that compacting a single FD stent may outperform deployment of two stents in producing additional reductions of the IR, AAV, and mean WSS.

The results of our systematic review confirmed that stent compaction and dual-stent deployment could both improve the flow diversion efficacy in terms of further reductions of IR (p<0.006) and AAV (p<0.02), which are both indicative of statistical significance. However, stent compaction did not demonstrate statistically significant further improvement of the TUT (p=0.08), in contrast to the deployment of an additional stent (p=0.02). This suggests that bulk hemodynamic parameters may be more prominently affected by a general increase in the stent wire density whereas localized parameters may be more sensitive to how the specific wire configuration was altered across an aneurysm orifice.

Furthermore, compacting a stent may be inappropriate when a patient has a highly curved recipient artery with an aneurysm

Table 2 Change of hemodynamic parameters (relative to the untreated condition) after deployment of an additional stent or when a single stent was deployed with a compaction technique applied compared with standard deployment of a single stent

	Hemodynamic parameters	No of studies	No of IAs	Mean difference	95% CI of difference	SD	P value
Overlapping	IR reduction (%)	4	7	−14.4	−19.6 to −9.3	5.6	0.0005*
	AAV reduction (%)	6	9	−16.8	−23.5 to −10.1	8.7	0.0004*
	WSS reduction (%)	4	6	−27.3	−31.4 to −23.3	3.9	<0.0001*
	TUT change (%)	2	4	47.0	11.3 to 82.7	22.4	0.0247†
Compaction	IR reduction (%)	4	8	−16.0	−25.4 to −6.7	11.3	0.0051†
	AAV reduction (%)	3	6	−23.3	−38.4 to −8.3	14.4	0.0105†
	TUT change (%)	2	4	58.3	−12.5 to 129.0	44.5	0.0791

*Statistical significance confirmed ($p<0.005$).
†Suggestive of statistical significance ($p<0.05$).
AAV, intra-aneurysmal average velocity; IA, intracranial aneurysm; IR, inflow rate; TUT, turnover time; WSS, wall shear stress.

located at the apex of the curvature. Zhang et al[18] pointed out that, in this circumstance, the stent wires might be pushed into the sac of an aneurysm due to the restoring force acting inside the wires, counter-productively resulting in a lower metal coverage ratio across the aneurysm orifice, causing treatment failure.

It should also be noted that enhancement of wire density through implantation of an additional stent may further impair patency of the side-branch arteries jailed by the implanted device.[25] Moreover, stent compaction or dual-stent deployment may increase the occurrence of post-treatment in-stent thrombosis, even when adequate dual antiplatelet therapy is administered.[26] This is still beyond the capability of numerical simulation to accurately predict. Therefore, although flow diversion can be improved through enhancement of stent wire density, whether these techniques can be applied must still take into consideration the patient-specific vascular conditions.

Uncertainties in virtual stent deployment and hemodynamic simulation

The simulation strategies reported in our surveyed studies were based on various combinations of modeling techniques, with few of them being able to be rigorously validated against clinical practice.

The primary factor limiting the fidelity of virtual stent deployment is that the wire configuration of stents deployed *in vivo* depends substantially on the skill, experience, and predilection of the treating clinicians, especially when a patient exhibits variation or tortuosity in vascular geometry, or for aneurysms with uncommon morphology in difficult-to-approach locations. Even under ideal vascular conditions, the landing position of the stent, the unsheathing process, and the pathway along which a stent is released can be quite different from the scenario modeled by virtual stent deployment.

In addition, only a limited number of studies have evaluated the local microscopic properties (eg, porosity and pore density) of stent wires at the aneurysm orifice. Such data would provide a better understanding of the efficacy of the stent in terms of aneurysmal IR and EL reduction in relation to specific vascular geometries with variations in diameter and curvature of the parent artery.

For analysis of the intra-aneurysmal hemodynamics, the key factors that may be detrimental to simulation accuracy are the adoption of generic vascular boundary conditions (eg, for flow rate and pressure) or the prescription of unphysiological velocity or pressure profiles at vascular openings. In most hemodynamic analyses, generalized inlet flow rates and outlet pressures—rather than patient-specific hemodynamic conditions—were

assumed. This may cause substantial under- or over-estimation of the actual flow diversion produced by a stent, as the aneurysmal inflow was reported to be linearly proportional to the strength of flow in the parent artery.[27 28] A recent study by Najafi et al[29] suggested that adoption of a cycle-average internal carotid artery flow rate derived from patient-specific phase-contrast MRI may help reduce error.

Furthermore, various assumptions were applied in hemodynamic simulation to simplify the description of blood flow (eg, assumption of a Newtonian fluid with constant viscosity and density). Saqr et al[30] recently concluded that the assumption of a Newtonian fluid may be invalid, especially when parameters quantifying the flow close to the vascular wall (eg, WSS) are to be assessed. Other simplifications include assuming the vascular wall to be rigid (ie, the wall would not deform over a cardiac cycle or even after implantation of a FD stent). However, Bouillot et al[31] have recently shown that deformation of the parent artery can be substantial after stent implantation, and Tupin et al[32] reported that the intra-aneurysmal flow pattern may be markedly affected by the compliance of the wall.

All these uncertainties and assumptions may lead to discrepancies between the *in vivo* aneurysmal hemodynamics and the simulated ones, yet the current imaging techniques lack the capability to capture the subtle *in vivo* flow patterns within an aneurysm, which could have been used as gold standard to regulate hemodynamic simulation. As a future direction, comprehensive validation and standardization of the protocols for virtual stent deployment and hemodynamic simulation would be useful, after which cogent results of virtual treatment may be used by clinicians in assessing the outcomes prior to real flow diversion treatment.

Limitations

Pursuant to the source studies, the present review has several limitations. The major one is that, although we have surveyed almost all studies ever published that reported post-treatment hemodynamics and aneurysm occlusion status, only five studies met our inclusion criteria for meta-analysis and even then most of the included studies had relatively small sample sizes. The reason is that performing virtual stent deployment and the subsequent hemodynamic analysis demands cutting-edge simulation skills and has a high resource intensity in terms of both manual interaction and computation time. Whether the conclusions drawn from our meta-analysis still hold for a larger group of aneurysm samples deserves further investigation.

The second inherent limitation is that the timepoints at which aneurysm occlusion status was observed varied from 3

to 12 months across the studies we included. Different research groups determined distinct endpoints following their local protocols for postoperative follow-ups. Although the criterion for classifying a treatment as successful was consistently specified as complete occlusion, lack of consistency among the specified observation times may potentially lead to misclassification of some treatment outcomes according to any single standard, thereby clouding exploration of the correlation between the hemodynamic and clinical outcomes.

Another limitation is that we have included two studies from the same group in our meta-analysis, which may potentially lead to duplicates of the included data. However, these two studies reported and focused on different hemodynamic parameters, and had different timepoints at which the status of aneurysm occlusion was assessed. Moreover, we failed to identify any overlapping cases through close examination of the aneurysm geometries.

CONCLUSION

Clinical outcomes following flow diversion treatment were found to be associated with the simulated aneurysm hemodynamics.

Differences in the post-treatment IR reduction (SMD -6.05, 95% CI -10.87 to -1.23, p=0.01) and EL reduction (SMD -5.28, 95% CI -7.09 to -3.46, p<0.001) between successfully and unsuccessfully treated patients were indicative of statistical significance, in contrast to the AAV (p=0.09), mean WSS (p=0.37), SR (p=0.09), and VCL (p=0.46). Deployment of stents with a compaction technique may yield additional enhancement of flow diversion comparable to that achieved through deployment of an additional stent.

Aneurysmal IR and EL have shown promise in discriminating between favorable and unfavorable patient outcomes following flow diversion treatments, pending future large studies into the diagnostic performance to establish the optimal cut-off thresholds.

Author affiliations
[1]Biomedical Flow Dynamics Laboratory, Tohoku University Institute of Fluid Science, Sendai, Miyagi, Japan
[2]Department of Neurosurgery, Saitama Medical University Saitama Medical Center, Kawagoe, Saitama, Japan
[3]Department of Mechanical and Electrical Engineering, Nagoya Institute of Technology, Nagoya, Aichi, Japan
[4]Division of Medical Devices, National Institute of Health Sciences, Kawasaki, Kanagawa, Japan
[5]Department of Neurosurgery, Mie Central Medical Center, Tsu, Mie, Japan
[6]Center for Advanced Biomedical Sciences (TWIns), Waseda University, Shinjuku, Tokyo, Japan
[7]Department of Innovation for Medical Information Technology, Jikei University School of Medicine, Minato, Tokyo, Japan
[8]Graduate School of Mechanical Engineering, Tokyo University of Science, Shinjuku, Tokyo, Japan
[9]ElyTMaX, CNRS – Université de Lyon – Tohoku University, International Joint Unit, Tohoku University, Sendai, Miyagi, Japan

Twitter Simon Tupin @SimonTupin

ORCID iDs
Mingzi Zhang http://orcid.org/0000-0002-0118-1160
Simon Tupin http://orcid.org/0000-0003-0982-8210
Yutaro Kohata http://orcid.org/0000-0002-4612-7440
Masaaki Shojima http://orcid.org/0000-0002-4388-151X
Makoto Ohta http://orcid.org/0000-0001-8571-6400

REFERENCES

1 Shobayashi Y, Tateshima S, Kakizaki R, et al. Intra-aneurysmal hemodynamic alterations by a self-expandable intracranial stent and flow diversion stent: high intra-aneurysmal pressure remains regardless of flow velocity reduction. *J Neurointerv Surg* 2013;5 Suppl 3:iii38–42.

2 Peach T, Spranger K, Ventikos Y. Virtual flow-diverter treatment planning: the effect of device placement on bifurcation aneurysm haemodynamics. *Proc Inst Mech Eng H* 2017;231:432–43.

3 Damiano RJ, Ma D, Xiang J, et al. Finite element modeling of endovascular coiling and flow diversion enables hemodynamic prediction of complex treatment strategies for intracranial aneurysm. *J Biomech* 2015;48:3332–40.

4 Sindeev S, Arnold PG, Frolov S, et al. Phase-contrast MRI versus numerical simulation to quantify hemodynamical changes in cerebral aneurysms after flow diverter treatment. *PLoS One* 2018;13:e0190696.

5 Kojima M, Irie K, Fukuda T, et al. The study of flow diversion effects on aneurysm using multiple enterprise stents and two flow diverters. *Asian J Neurosurg* 2012;7:159–65.

6 Radaelli AG, Augsburger L, Cebral JR, et al. Reproducibility of haemodynamical simulations in a subject-specific stented aneurysm model--a report on the Virtual Intracranial Stenting Challenge 2007. *J Biomech* 2008;41:2069–81.

7 Cebral JR, Mut F, Raschi M, et al. Analysis of hemodynamics and aneurysm occlusion after flow-diverting treatment in rabbit models. *AJNR Am J Neuroradiol* 2014;35:1567–73.

8 Paliwal N, Jaiswal P, Tutino VM, et al. Outcome prediction of intracranial aneurysm treatment by flow diverters using machine learning. *Neurosurg Focus* 2018;45:E7.

9 Chong W, Zhang Y, Qian Y, et al. Computational hemodynamics analysis of intracranial aneurysms treated with flow diverters: correlation with clinical outcomes. *AJNR Am J Neuroradiol* 2014;35:136–42.

10 Tsang ACO, Lai SSM, Chung WC, et al. Blood flow in intracranial aneurysms treated with pipeline embolization devices: computational simulation and verification with Doppler ultrasonography on phantom models. *Ultrasonography* 2015;34:98–108.

11 Cancelliere NM, Nicholson P, Radovanovic I, et al. Comparison of intra-aneurysmal flow modification using optical flow imaging to evaluate the performance of Evolve and Pipeline flow diverting stents. *J Neurointerv Surg* 2020;12:814–7.

12 Kulcsár Z, Augsburger L, Reymond P, et al. Flow diversion treatment: intra-aneurismal blood flow velocity and WSS reduction are parameters to predict aneurysm thrombosis. *Acta Neurochir* 2012;154:1827–34.

13 Mut F, Raschi M, Scrivano E, et al. Association between hemodynamic conditions and occlusion times after flow diversion in cerebral aneurysms. *J Neurointerv Surg* 2015;7:286–90.

14 Chung B, Mut F, Kadirvel R, *et al*. Hemodynamic analysis of fast and slow aneurysm occlusions by flow diversion in rabbits. *J Neurointerv Surg* 2015;7:931–5.

15 Peach TW, Ngoepe M, Spranger K, *et al*. Personalizing flow-diverter intervention for cerebral aneurysms: from computational hemodynamics to biochemical modeling. *Int J Numer Method Biomed Eng* 2014;30:1387–407.

16 Paliwal N, Damiano RJ, Davies JM, *et al*. Association between hemodynamic modifications and clinical outcome of intracranial aneurysms treated using flow diverters. *Proc SPIE Int Soc Opt Eng* 2017;10135:101352F.

17 Berg P, Saalfeld S, Janiga G, *et al*. Virtual stenting of intracranial aneurysms: a pilot study for the prediction of treatment success based on hemodynamic simulations. *Int J Artif Organs* 2018;41:698–705.

18 Zhang M, Li Y, Zhao X, *et al*. Haemodynamic effects of stent diameter and compaction ratio on flow-diversion treatment of intracranial aneurysms: a numerical study of a successful and an unsuccessful case. *J Biomech* 2017;58:179–86.

19 Li Y, Zhang M, Verrelli DI, *et al*. Numerical simulation of aneurysmal haemodynamics with calibrated porous-medium models of flow-diverting stents. *J Biomech* 2018;80:88–94.

20 Ma D, Dumont TM, Kosukegawa H, *et al*. High fidelity virtual stenting (HiFiVS) for intracranial aneurysm flow diversion: in vitro and in silico. *Ann Biomed Eng* 2013;41:2143–56.

21 Raschi M, Mut F, Löhner R, *et al*. Strategy for modeling flow diverters in cerebral aneurysms as a porous medium. *Int J Numer Method Biomed Eng* 2014;30:909–25.

22 Damiano RJ, Tutino VM, Paliwal N, *et al*. Compacting a single flow diverter versus overlapping flow diverters for intracranial aneurysms: a computational study. *AJNR Am J Neuroradiol* 2017;38:603–10.

23 Taylor JR. *Introduction to error analysis: the study of uncertainties in physical measurements*. University Science Books, 1997.

24 Shapiro M, Raz E, Becske T, *et al*. Variable porosity of the pipeline embolization device in straight and curved vessels: a guide for optimal deployment strategy. *AJNR Am J Neuroradiol* 2014;35:727–33.

25 Iosif C, Berg P, Ponsonnard S, *et al*. Role of terminal and anastomotic circulation in the patency of arteries jailed by flow-diverting stents: from hemodynamic changes to ostia surface modifications. *J Neurosurg* 2017;126:1702–13.

26 Alderazi YJ, Shastri D, Kass-Hout T, *et al*. Flow diverters for intracranial aneurysms. *Stroke Res Treat* 2014;2014:1–12.

27 Morales HG, Bonnefous O, Geers AJ, *et al*. Does arterial flow rate affect the assessment of flow-diverter stent performance? *AJNR Am J Neuroradiol* 2016;37:2293–8.

28 Chnafa C, Bouillot P, Brina O, *et al*. Errors in power-law estimations of inflow rates for intracranial aneurysm CFD. *J Biomech* 2018;80:159–65.

29 Najafi M, Cancelliere NM, Brina O, *et al*. How patient-specific do internal carotid artery inflow rates need to be for computational fluid dynamics of cerebral aneurysms? *J Neurointerv Surg* 2020:neurintsurg-2020-015993.

30 Saqr KM, Rashad S, Tupin S, *et al*. What does computational fluid dynamics tell us about intracranial aneurysms? A meta-analysis and critical review. *J Cereb Blood Flow Metab* 2020;40:1021–39.

31 Bouillot P, Brina O, Yilmaz H, *et al*. Virtual-versus-real implantation of flow diverters: clinical potential and influence of vascular geometry. *AJNR Am J Neuroradiol* 2016;37:2079–86.

32 Tupin S, Saqr KM, Ohta M. Effects of wall compliance on multiharmonic pulsatile flow in idealized cerebral aneurysm models: comparative PIV experiments. *Exp Fluids* 2020;61:164.

33 Paliwal N, Yu H, Xu J, *et al*. Virtual stenting workflow with vessel-specific initialization and adaptive expansion for neurovascular stents and flow diverters. *Comput Methods Biomech Biomed Engin* 2016;19:1423–31.

34 Appanaboyina S, Mut F, Löhner R, *et al*. Computational fluid dynamics of stented intracranial aneurysms using adaptive embedded unstructured grids. *Int J Numer Methods Fluids* 2008;57:475–93.

35 Augsburger L, Reymond P, Rufenacht DA, *et al*. Intracranial stents being modeled as a porous medium: flow simulation in stented cerebral aneurysms. *Ann Biomed Eng* 2011;39:850–63.

Supplemental material

BMJ Publishing Group Limited (BMJ) disclaims all liability and responsibility arising from any reliance placed on this supplemental material which has been supplied by the author(s)

J NeuroIntervent Surg

Supplementary Material 1

This supplementary material presents the lists of studies respectively included in the Quantitative Analysis (A) and (B).
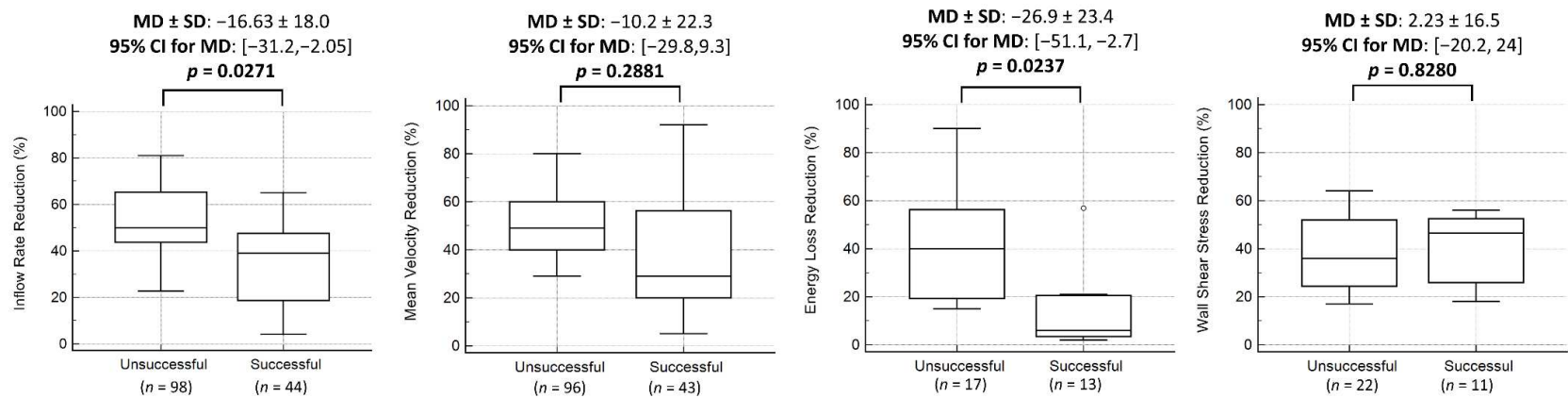
I. List of studies included in Quantitative Analysis (A)

Berg, P. et al. (2018) 'Virtual stenting of intracranial aneurysms: A pilot study for the prediction of treatment success based on hemodynamic simulations', *The International Journal of Artificial Organs*, 41(11), pp. 698–705. doi: 10.1177/0391398818775521.

Chong, W. et al. (2014) 'Computational hemodynamics analysis of intracranial aneurysms treated with flow diverters: correlation with clinical outcomes', *American Journal of Neuroradiology*, 35(1), pp. 136–142. doi: 10.3174/ajnr.A3790.

Karmonik, C. et al. (2013) 'Hemodynamics at the ostium of cerebral aneurysms with relation to post-treatment changes by a virtual flow diverter: a computational fluid dynamics study', in *Conference proceedings: ... Annual International Conference of the IEEE Engineering in Medicine and Biology Society. IEEE Engineering in Medicine and Biology Society. Annual Conference*, pp. 1895–1898. doi: 10.1109/EMBC.2013.6609895.

Kulcsár, Z. et al. (2012) 'Flow diversion treatment: intra-aneurismal blood flow velocity and WSS reduction are parameters to predict aneurysm thrombosis', *Acta Neurochirurgica*, 154(10), pp. 1827–1834. doi: 10.1007/s00701-012-1482-2.

Li, Y. et al. (2018) 'Numerical simulation of aneurysmal haemodynamics with calibrated porous-medium models of flow-diverting stents', *Journal of Biomechanics*, 80, pp. 88–94. doi: 10.1016/j.jbiomech.2018.08.026.

Mut, F. et al. (2015) 'Association between hemodynamic conditions and occlusion times after flow diversion in cerebral aneurysms', *Journal of Neurointerventional Surgery*, 7(4), pp. 286–290. doi: 10.1136/neurintsurg-2013-011080.

Paliwal, N. et al. (2017) 'Association between hemodynamic modifications and clinical outcome of intracranial aneurysms treated using flow diverters', in Webster, R. J. and Fei, B. (eds). *SPIE Medical Imaging*, Orlando, Florida, United States, p. 101352F. doi: 10.1117/12.2254584.

Paliwal, N. et al. (2018) 'Outcome prediction of intracranial aneurysm treatment by flow diverters using machine learning', *Neurosurgical Focus*, 45(5), p. E7. doi: 10.3171/2018.8.FOCUS18332.

Sindeev, S. et al. (2018) 'Phase-contrast MRI versus numerical simulation to quantify hemodynamical changes in cerebral aneurysms after flow diverter treatment', *PloS One*, 13(1), p. e0190696. doi: 10.1371/journal.pone.0190696.

Xiang, J. et al. (2015) 'High-fidelity virtual stenting: modeling of flow diverter deployment for hemodynamic characterization of complex intracranial aneurysms', *Journal of Neurosurgery*, 123(4), pp. 832–840. doi: 10.3171/2014.11.JNS14497.

Zhang, M. et al. (2017) 'Haemodynamic effects of stent diameter and compaction ratio on flow-diversion treatment of intracranial aneurysms: A numerical study of a successful and an unsuccessful case', *Journal of Biomechanics*, 58, pp. 179–186. doi: 10.1016/j.jbiomech.2017.05.001.

Zhang, Y., Chong, W. and Qian, Y. (2013) 'Investigation of intracranial aneurysm hemodynamics following flow diverter stent treatment', *Medical Engineering & Physics*, 35(5), pp. 608–615. doi: 10.1016/j.medengphy.2012.07.005.

1

## II. List of studies included in Quantitative Analysis (B)

Damiano, R. J. et al. (2015) 'Finite element modeling of endovascular coiling and flow diversion enables hemodynamic prediction of complex treatment strategies for intracranial aneurysm', *Journal of Biomechanics*, 48(12), pp. 3332–3340. doi: 10.1016/j.jbiomech.2015.06.018.

Damiano, R. J. et al. (2017) 'Compacting a Single Flow Diverter versus Overlapping Flow Diverters for Intracranial Aneurysms: A Computational Study', *American Journal of Neuroradiology*, 38(3), pp. 603–610. doi: 10.3174/ajnr.A5062.

Janiga, G. et al. (2015) 'An automatic CFD-based flow diverter optimization principle for patient-specific intracranial aneurysms', *Journal of Biomechanics*, 48(14), pp. 3846–3852. doi: 10.1016/j.jbiomech.2015.09.039.

Li, Y. et al. (2018) 'Numerical simulation of aneurysmal haemodynamics with calibrated porous-medium models of flow-diverting stents', *Journal of Biomechanics*, 80, pp. 88–94. doi: 10.1016/j.jbiomech.2018.08.026.

Ma, D. et al. (2014) 'Enhanced aneurysmal flow diversion using a dynamic push-pull technique: an experimental and modeling study', *American Journal of Neuroradiology*, 35(9), pp. 1779–1785. doi: 10.3174/ajnr.A3933.

Uchiyama, Y. et al. (2018) 'Hemodynamic Change In A Cerebral Aneurysm Treated By Double Stenting Technique', in *2018 40th Annual International Conference of the IEEE Engineering in Medicine and Biology Society (EMBC). 2018 40th Annual International Conference of the IEEE Engineering in Medicine and Biology Society (EMBC)*, Honolulu, HI: IEEE, pp. 1343–1346. doi: 10.1109/EMBC.2018.8512461.

Ugron, A., Szikora, I. and Paál, G. (2014) 'Measurement of flow diverter hydraulic resistance to model flow modification in and around intracranial aneurysms', *Interventional Medicine & Applied Science*, 6(2), pp. 61–68. doi: 10.1556/IMAS.6.2014.2.2.

Wang, C. et al. (2016) 'Flow diverter effect of LVIS stent on cerebral aneurysm hemodynamics: a comparison with Enterprise stents and the Pipeline device', *Journal of Translational Medicine*, 14(1), p. 199. doi: 10.1186/s12967-016-0959-9.

Xiang, J. et al. (2014) 'Increasing flow diversion for cerebral aneurysm treatment using a single flow diverter', *Neurosurgery*, 75(3), pp. 286–294; discussion 294. doi: 10.1227/NEU.0000000000000409.

Xiang, J. et al. (2015) 'High-fidelity virtual stenting: modeling of flow diverter deployment for hemodynamic characterization of complex intracranial aneurysms', *Journal of Neurosurgery*, 123(4), pp. 832–840. doi: 10.3171/2014.11.JNS14497.

Zhang, M. et al. (2017) 'Haemodynamic effects of stent diameter and compaction ratio on flow-diversion treatment of intracranial aneurysms: A numerical study of a successful and an unsuccessful case', *Journal of Biomechanics*, 58, pp. 179–186. doi: 10.1016/j.jbiomech.2017.05.001.

Supplemental material

BMJ Publishing Group Limited (BMJ) disclaims all liability and responsibility arising from any reliance placed on this supplemental material which has been supplied by the author(s)

J NeuroIntervent Surg

Supplementary Figure 1

Supplementary Figure 1. Comparison of haemodynamic changes between the successfully and unsuccessfully treated cases, in terms of (1) the inflow rate, (2) intra-aneurysmal velocity, (3) energy loss, and (4) wall shear stress, all relative to the untreated condition. n refers to the number of aneurysms included in each comparison group. MD: mean difference; SD: standard deviation; and CI: confidence interval. The boxplots present the minimum, first quartile, median, third quartile, and maximum (excluding outliers) of each such dataset, with an orange circle indicating the outlier.

1

Supplementary Figure 2
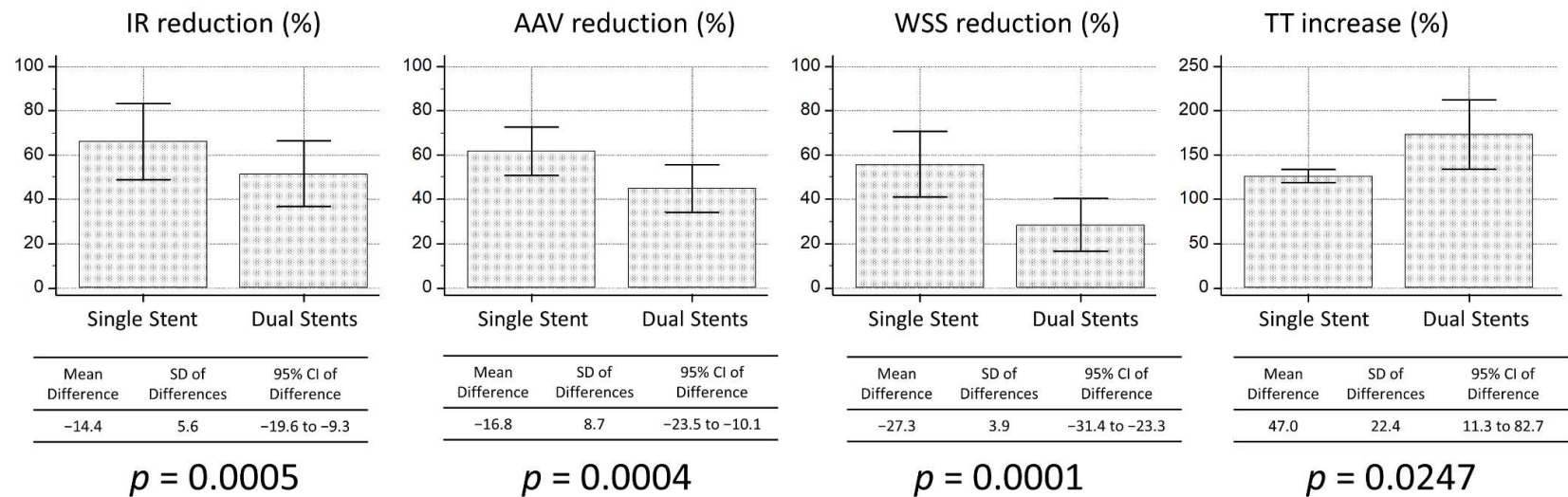
Supplementary Figure 2. Comparison of haemodynamic differences between treatments using a single stent and using two overlapping stents, in terms of (1) the inflow rate, (2) intra-aneurysmal velocity, (3) wall shear stress, and (4) turnover time, all relative to the untreated condition. SD: standard deviation; and CI: confidence interval. Error bars indicate the standard deviation of each dataset.

2

Supplemental material

BMJ Publishing Group Limited (BMJ) disclaims all liability and responsibility arising from any reliance placed on this supplemental material which has been supplied by the author(s)

J NeuroIntervent Surg

Supplementary Figure 3
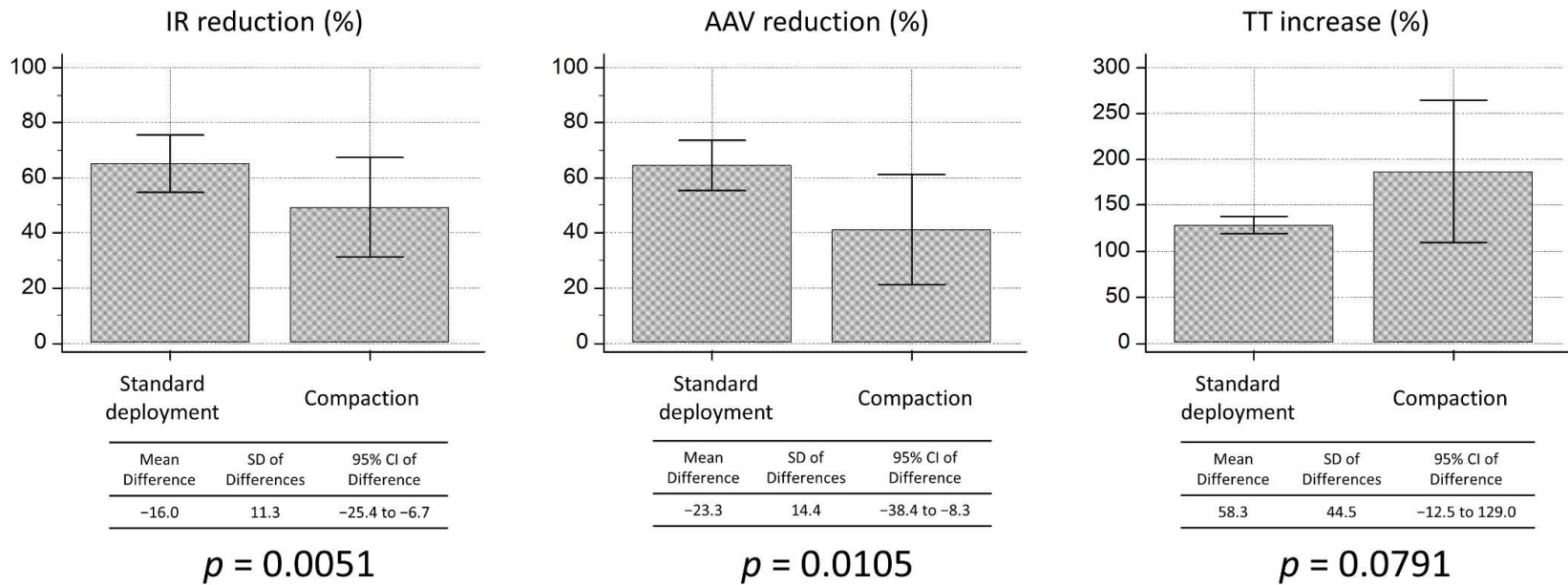
Supplementary Figure 3. Comparison of haemodynamic differences between standard deployment of a FD stent and deployment with a compaction technique applied, in terms of (1) the inflow rate, (2) intra-aneurysmal velocity, and (3) turnover time, all relative to the untreated condition. SD: standard deviation; and CI: confidence interval. Error bars indicate the standard deviation of each dataset.

3

Supplemental material

BMJ Publishing Group Limited (BMJ) disclaims all liability and responsibility arising from any reliance placed on this supplemental material which has been supplied by the author(s)

J NeuroIntervent Surg

Supplementary Table 1

Supplementary Table 1. Information on studies included in the quantitative analysis for differences between the single- and dual-stent treatments, and between deployments with and without a compaction technique applied.

Author, year	Number of aneurysms	Location of aneurysms	Types of aneurysm	Aspect ratios (mean)	FD stent model	Virtual stenting technique	Multiple FD stents deployed	Compaction technique applied
Li et al., 2018	2	ICA	SW		*PED*	Porous medium	*	
Uchiyama et al., 2018	1	ICA	SW		*PED*	Generalised Cylinder	*	
Zhang et al., 2017	2	ICA	SW		*Silk*	Spring–mass		*
Damiano et al., 2017	3	1 BT, 2 ICA	1 FU, 2 SW		*PED*	Finite Element Analysis	*	*
Wang et al., 2016	3	ICA	SW	1.56	*PED*	Simplex	*	
Xiang et al., 2015	4	1 VA, 3 ICA	1 FU, 3 SW	1.32	*PED*	Finite Element Analysis	*	
Damiano et al., 2015	1	ICA	SW		*PED*	Finite Element Analysis	*	
Janiga et al., 2015	1	ICA	SA	1.10	*Silk*	Generalised Cylinder		*
Ugron et al., 2014	2	ICA	SW	1.55	*PED*	Porous medium	*	
Xiang et al., 2014	1	BT	SW		*PED*	Finite Element Analysis		*
Ma et al., 2014	2	1 ACA, 1 BT	1 FU, 1 SW	2.14	*PED*	Finite Element Analysis		*

ICA: internal carotid artery; BT: basilar trunk; VA: vertebral artery; ACA: anterior cerebral artery; SW: side-wall; and FU: fusiform.

Haemodynamic data summarised from those studies are presented in Supplementary Table 2.

4

Supplementary Table 2

Supplementary Table 2. Summary of haemodynamic changes (relative to the untreated condition) after deployment of an additional stent or when a single stent was deployed with a compaction technique applied, in comparison to standard deployment of a single stent.

Author, year	Multiple FD stents deployed	Compaction technique applied	IR reduction (%)		AAV reduction (%)		WSS reduction (%)		EL reduction (%)		TUT increase (%)	
			S-MCR	*H-MCR*	*S-MCR*	*H-MCR*	*S-MCR*	*H-MCR*	*S-MCR*	*H-MCR*	*S-MCR*	*H-MCR*
Li et al., 2018	*		35	25					4	2		
"			45	35					17	11		
Uchiyama et al., 2018	*				71	58						
Zhang et al., 2017		*	45	10	55	20			20	2		
"			65	40	65	40			40	15		
Damiano et al., 2017		*	70	50	60	30	55	15			130	220
"		*	82	78	80	70	77	50			120	140
"		*	70	68	60	58	45	57			130	150
"	*				60		50	30				160
"	*				60		61	42				160
"	*				50		30	18				210
Wang et al., 2016	*				60	45	50	25				
Xiang et al., 2016	*		80	61	80	61	68	42			125	163
Damiano et al., 2015	*		80	70	60	30	40	15				
"					60		20	10†				
Janiga et al., 2015		*			76	67						
Ugron et al., 2014	*				38	25						
"					50	45						
Xiang et al., 2015		*			67	29					134	237
Ma et al., 2014		*	64	43								
"			50	38								

IR: inflow rate; AAV: intra-aneurysmal average velocity; WSS: wall shear stress; EL: energy loss; TUT: turnover time; S-MCR: standard metal coverage ratio (following treatment with a single stent deployed in a standard manner); and H-MCR: higher metal coverage ratio (following treatment using two stents or treatment using a single stent deployed with a compaction technique applied).

5

Supplementary Material 2

This supplementary material presents methods and results of analysis of the correlations between four haemodynamic parameters and clinical treatment outcomes through use of a binary logistic regression model.

Method:

A binary logistic regression model was constructed to evaluate the relationship between flow-diversion outcome (*i.e.* aneurysm occlusion) and each of the four haemodynamic parameters — IR, EL, AAV, and WSS. Calibration of the model (*i.e.* statistical precision) was assessed by the Hosmer-Lemeshow goodness-of-fit test, with $p > 0.05$ being an indication of that the model has a high predictive ability (*i.e.* no statistical difference between observed and expected values). All analyses were performed using MedCalc version 19.1 (Ostend, Belgium).

Results:

Figure S2-1 shows the logistic regression curves corresponding to the four haemodynamic parameters investigated, and **Table S2-1** presents the statistical results of each analysis. Logistic regression analyses revealed that IR (OR: 0.9468, 95% CI: 0.8976 to 0.9987, $p = 0.0208$) and EL (OR: 0.9389, 95% CI: 0.8766 to 1.0057, $p = 0.0171$) better predict aneurysm occlusion, in contrast to AAV ($p = 0.2628$) and WSS ($p = 0.8075$), which is in agreement with the findings of our meta-analysis.
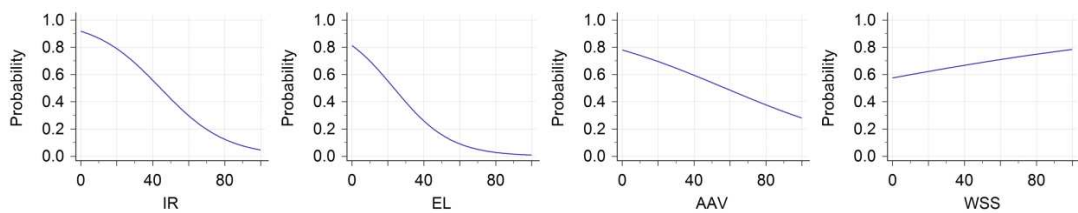

Figure S2-1. Binary logistic regression curves of IR, EL, AAV, and WSS in relation to the clinical outcomes after flow-diversion intervention. IR: inflow rate; EL: energy loss; AAV: intra-aneurysmal average velocity; and WSS: wall shear stress.

Table S2-1. Statistical results of the logistic regression of four haemodynamic parameters.

| Parameters | Coeff. | SE | Wald | *p* value | Hosmer & Lemeshow test | | OR | 95% CI of OR |
					χ^2	*p* value		
IR	-0.0546	0.0272	4.0292	**0.0208**†	6.3114	0.5039	0.9468	0.8976 to 0.9987
EL	-0.0630	0.0350	3.2324	**0.0171**†	7.6540	0.3641	0.9389	0.8766 to 1.0057
AAV	-0.0221	0.0204	1.1749	0.2628	15.7943	**0.0454**†	0.9781	0.9397 to 1.0180
WSS	0.0099	0.0407	0.0592	0.8075	7.3651	0.1178	1.0100	0.9325 to 1.0939

IR: inflow rate; EL: energy loss; AAV: intra-aneurysmal average velocity; WSS: wall shear stress; Coeff.: coefficient; SE: standard error; OR: odds ratio; and CI: confidence interval.

† suggestive of statistical significance ($p < 0.05$).

1